

Performance of the coupled-cluster singles and doubles method applied to two-dimensional quantum dots

E. Waltersson, C. J. Wesslén, and E. Lindroth

Department of Physics, Stockholm University, AlbaNova, S-106 91 Stockholm, Sweden

(Received 28 August 2012; revised manuscript received 1 November 2012; published 9 January 2013)

An implementation of the coupled-cluster single and double excitations (CCSD) method on two-dimensional quantum dots is presented. Advantages and limitations are studied through comparison with other high accuracy approaches, including another CCSD implementation, for up to twelve confined electrons. The possibility to effectively use a very large basis set is found to be an important advantage compared to full configuration interaction implementations. The error in the ground-state energy introduced by truncating at triple excitations is shown to be comparable to the difference between the results from the variation and diffusion Monte Carlo methods. Convergence of the iterative solution of the coupled cluster equations is found for surprisingly weak confinement strengths even when the full electron-electron interaction is treated as a perturbation. The relevance of the omitted excitations is investigated through comparison with full configuration interaction results.

DOI: [10.1103/PhysRevB.87.035112](https://doi.org/10.1103/PhysRevB.87.035112)

PACS number(s): 73.21.La, 71.15.-m, 31.15.bw

I. INTRODUCTION

Ever since Tarucha *et al.*¹ experimentally demonstrated atomlike properties in few electron quantum dots, in particular the existence of a shell structure, these systems have attracted a lot of theoretical interest as new targets for many-body methods. In contrast to the situation for the naturally occurring many-body systems, the strength of the overall confinement relative to that of the interparticle interaction can here be freely varied over a large range and thus completely new regimes can be explored. When the aim is to study the performance of a specific many-body method, it is justified to use a simple model for the confining potential and many theoretical studies restrict themselves to the two-dimensional harmonic oscillator potential. The interaction between the dot electrons and the surrounding semiconductor material is further usually modeled through the use of a material specific effective electron mass and relative dielectric constant. This model implies thus a two-dimensional truly atomlike device on which calculation methods developed for atoms can be applied after minor adjustments. Early calculations proved the model to be adequate. Combined with a reasonable account for the electron-electron interaction through methods such as density functional theory (DFT)²⁻⁶ or Hartree-Fock,⁷⁻¹⁰ the two-dimensional harmonic oscillator confining potential did indeed give a good qualitative agreement with experiments. In particular, the closed shells forming with two, six, and twelve trapped electrons could be explained, as shown in many studies, see, e.g., the review by Reimann and Manninen.¹¹

Neither the true form of the dot confinement nor the extent to which it deviates from being purely two dimensional is easily extracted from experiments. To correctly describe an experimental situation, a theoretical model has thus to account both for the form of the exterior potential as well as the internal many-body effects in the dot. The theoretical model presented in this paper focuses on the properties of the internal interactions in the confined system. If the many-body problem can be adequately solved, it is later only a question of tuning the form of the external confinement potential, to fit specific experimentally created dots. This would then also open for

a better understanding of their properties. Some studies in this direction have been performed, e.g., by Matagne *et al.*¹² who made quantitative statements about the nonharmonicity of the confining potential from the comparison between DFT calculations and experiments. DFT has proven to be able to account for a large part of the electron correlation, but still it is not really the best choice for such investigations since it is hard to make an a priori estimate of the obtained error. There are several ways to account for correlation more systematically. A number of studies on quantum dots and related structures have been carried out with configuration interaction (CI), see, e.g., Refs. 13–22. Full CI is, in principle, exact and applicable for all relative interaction strengths. The term “full CI” refers to a calculation where all Slater determinants, obtained by exciting all possible electrons to all possible orbitals that are unoccupied in the studied electronic configuration, are included. It is obvious that the size of the full CI problem grows extremely fast both with the number of particles and with the size of the basis set (used to represent the unoccupied orbitals). It is well known that truncated CI, i.e., keeping, e.g., only single and double excitations from the leading configuration, lacks size extensivity. In short, this implies that the method does not scale properly with the size of the studied system, see, for example, the review by Bartlett.²³ Truncation of the number of excitations is thus not a real option, and instead, all but the smallest systems have to be calculated with very small basis sets. Recently, a thorough investigation of the performance of full CI applied to quantum dots with a basis set consisting of harmonic oscillator eigenfunctions was made by Kvaal²¹ and the main conclusion was that the convergence with respect to the size of the basis set was slow and that additional features such as effective two-body interactions have to be added for meaningful comparisons with experiments. An alternative approach for high-accuracy calculations is quantum Monte Carlo (QMC) methods, which successfully have been applied to quantum dots.²⁴⁻³² Here, the computational cost grows modestly with the number of electrons, and the method provides a very efficient way to calculate the ground state for a specific symmetry. The nodal structure of the trial wave function can be used to impose

restrictions on the solutions so that also excited states can be obtained to some extent, see, e.g., the discussion in the review by Foulkes *et al.*³³ Still, calculations on general excited states are not straightforward and additional methods are needed for realistic calculations on important parts of the quantum dot spectrum.

Most of the methods used on atoms and molecules have also been applied to quantum dots in several implementations. The least studied method is however many-body perturbation theory which has been shown to be very powerful for the calculation of atomic properties. Calculations up to second order in the perturbation expansion have been made by just a few authors,^{34,35} and equally few coupled-cluster calculations have been presented.^{36–38} For small to medium sized molecules as well as atoms, the coupled-cluster(CC) method is known to successfully combine feasibility with accuracy. The coupled-cluster theory was introduced in 1960 by Coester and Kümmel³⁹ in nuclear physics, and since then contributions have been given by many authors. A review regarding its performance in quantum chemistry has been made by Bartlett and Musiał.⁴⁰ We present here a thorough investigation of how the coupled-cluster method with single and double excitations (CCSD) performs, in comparison with full CI and quantum Monte Carlo studies, on two-dimensional quantum dots. In Sec. II, we summarize CCSD and briefly discuss its advantages. In Sec. III, our implementation for calculations on circular quantum dots is outlined. In Sec. IV, we present results for dots with up to twelve electrons and compare them with those obtained with other methods as well as a comparison to another CCSD implementation.³⁸ The first question is whether the restriction to single and double excitations is adequate. It is known to be a good approximation for atoms, but we expect it to eventually fail for sufficiently weak confinement strengths. Here, we try to establish when this happens. The next point is the feasibility and we show that results converged with respect to, e.g., basis size can be obtained for much larger systems than is possible for CI calculations. We show for $\hbar\omega \sim 3$ meV and the $N = 2$ to 8 ground states that the error relative to diffusion Monte Carlo results is in the range of a few tenths of a percent. Said system has been chosen in other theoretical studies, e.g., Pederiva,²⁷ to approximate the quantum dots investigated experimentally by Tarucha *et al.*¹ An attempt to extrapolate results for even larger basis sets in order to increase accuracy even further is also presented.

II. THEORY

The formalism used in the present study can be found in more detail in the textbook by Lindgren and Morrison.⁴¹ Here, we just discuss the important aspects required for understanding of the present results. In order to solve the Schrödinger equation,

$$H\Psi = E\Psi, \quad (1)$$

for an N -fermion system, the Hamiltonian is partitioned as

$$H = H_0 + V, \quad (2)$$

where the eigenstates of H_0 are known and V is the remainder, i.e., it is the perturbation with respect to the already solved

Hamiltonian H_0 . In the present study, H_0 is usually the Hamiltonian for the noninteracting system, and thus V is the whole electron-electron interaction, but also other choices have been examined as will be discussed below. We will further assume that H_0 is a sum of N single-particle Hamiltonians with known eigenstates:

$$H_0 = \sum_i^N h_i, \quad h_i |i\rangle = \varepsilon_i |i\rangle, \quad (3)$$

where the orbitals, $|i\rangle$, form a *model space* suitable for the states of interest. In the following, we will use a one-dimensional model space P spanned by one Slater determinant:

$$\alpha = \{abcd \dots N\}, \quad (4)$$

$$P = |\alpha\rangle\langle\alpha|, \quad (5)$$

where a, b, c, d, \dots, N denote the occupied orbitals, and the curly brackets denote anti-symmetrization. A multidimensional *extended* model space is also a possibility,⁴¹ but this will be left for future investigations. The *model function* is the projection of the exact solution, Eq. (1), onto the model space:

$$\Psi_0 = P\Psi. \quad (6)$$

We further assume that the model function is normalized, a condition usually referred to as *intermediate normalization*. It is possible to define a *wave operator*, Ω that transforms the model function into the exact state, i.e., $\Psi = \Omega\Psi_0$. In order to separate the part of Ω that projects onto the model space from that which brings the solution out of the model space, we write

$$\Omega = 1 + \chi, \quad (7)$$

where χ is sometimes referred to as the correlation operator. The wave operator can be obtained from the *generalized Bloch equation*, which we will use in the form^{41–43}

$$[\Omega, H_0]P = (QV\Omega P - \chi P V \Omega P), \quad (8)$$

where Q is the orthogonal space to P , such that $P + Q = 1$. Equation (8) is equivalent to the Schrödinger equation, but in this form, it allows for an iterative solution procedure. Setting χ on the right-hand side initially to zero, one can obtain a first approximation of χ , which then can be inserted on the right-hand side to get a better approximation and so on until convergence is reached. When an order by order expansion is carried through, it can be shown that in each order the so called *unlinked* diagrams from the first term in Eq. (8) are canceled by contributions from the second term. Unlinked contributions are those that include parts that are surrounded by P operators, as the $\chi P V \Omega P$ term in Eq. (8). This is the so-called *linked diagram theorem*, see, for example, Refs. 41 and 40 and references therein. It is thus possible to keep only linked contributions in the expansion, and it is this linked expansion that will be the basis for the coupled cluster expansion below.

When Ω has been obtained, it can be used to construct the *effective Hamiltonian*

$$H_{\text{eff}} = P H_0 P + P V \Omega P, \quad (9)$$

which gives the exact energies when acting on the model space.⁴¹ The total energy can then be written as

$$E = \langle \alpha | H_{\text{eff}} | \alpha \rangle = \langle \alpha | H_0 + V + V \chi | \alpha \rangle, \quad (10)$$

where $P | \alpha \rangle = | \alpha \rangle$ has been used. We see now from Eq. (9) that the last term in Eq. (8) can be understood as the energy correction ($PV\Omega P$) times the correction to the wave function, given by χ . In both these parts, there will be a sum over all particles. The cancellation of all unlinked diagrams, mentioned above, occurs only if the sum over particles runs independently also for disconnected parts of the first term in Eq. (8), i.e., in $QV\Omega P$. There will then be individual contributions where the exclusion principle appears to be violated, but since antisymmetrization is strictly enforced this does not introduce any unphysical contributions in the result. This issue has been discussed by several authors, see, e.g., Ref. 40.

The complementary space Q , orthogonal to P , can formally be built up from all Slater determinants β that differ from α :

$$Q = \sum_{\beta \neq \alpha} | \beta \rangle \langle \beta |. \quad (11)$$

The space spanned by Q is, in principle, infinite, but in practice, we use a finite basis set to represent the eigenstates to h , Eq. (3). This makes also the Q space finite, but still it grows rapidly both with the size of the basis set and with the number of particles. We focus now on the representation of the Q space for several particles. For this purpose, we can classify the Slater determinants belonging to Q with respect to by how many single particles states they differ from P . For example,

$$\alpha_a^r = \{ r b c d \dots N \}, \quad (12)$$

differs from Eq. (4) only in that a has been replaced by r , and it is labeled a *single* excitation, while

$$\alpha_{ab}^{rs} = \{ r s c d \dots N \}, \quad (13)$$

differs from Eq. (4) in that a and b have been replaced by r and s , and it is labeled a *double* excitation. A complete calculation on a two-particle system requires single and double excitations, while such a calculation on a three particle system also requires triple excitations, and so on. For a general many-particle system, it is necessary to truncate this series at some point due to both complexity and computational load. For this truncation, there exists several choices. χ , the part of the wave operator that lies in the Q space, can for example be divided up as

$$\chi = \chi_1 + \chi_2 + \chi_3 + \dots, \quad (14)$$

where the subscripts denote the number of excitations. If we truncate this sum after, e.g., χ_3 , we will reproduce CI with single, double, and triple excitations.⁴⁰ With the coupled-cluster approach the truncation is made in an alternative way. First, we start from the linked form of the Bloch equation,

$$[\Omega, H_0] P = (QV\Omega P - \chi PV\Omega P)_{\text{linked}}, \quad (15)$$

where only linked contributions are retained in the iterative procedure. As a second step we define a *cluster operator* $S = S_1 + S_2 + S_3 + \dots$, where each term represents the *connected* part of the wave operator for n excitations, $S_n = (\Omega_n)_{\text{connected}}$. The term connected denotes that the wave operator cannot be

divided up in parts where the particles interact independently in smaller clusters, e.g., two by two. The S operator can be shown to satisfy a Bloch type equation⁴⁴

$$[S, H_0] P = (QV\Omega P - \chi PV\Omega P)_{\text{connected}}. \quad (16)$$

The wave operator Ω can now be written as a sum of products of S_n operators. All such terms are generated through the *exponential ansatz*:

$$\begin{aligned} \Omega = \{ \exp(S) \} &= 1 + S_1 + S_2 + \frac{1}{2!} \{ S_1 \}^2 + \{ S_1 S_2 \} + \frac{1}{3!} \{ S_1 \}^3 \\ &+ \frac{1}{2!} \{ S_2 \} + \frac{1}{2!} \{ S_1^2 S_2 \} + \frac{1}{4!} \{ S_1 \}^4 + \dots \end{aligned} \quad (17)$$

The curly brackets denote here that it is the normal ordered products of the operators that should be used, which implies antisymmetrization. We can now identify all single, double, triple, etc., excitations accordingly:

$$\begin{aligned} \Omega_1 &= \boxed{S_1}, \\ \Omega_2 &= \boxed{S_2 + \frac{1}{2} \{ S_1^2 \}}, \\ \Omega_3 &= S_3 + \boxed{\{ S_1 S_2 \} + \frac{1}{3!} \{ S_1 \}^3}, \\ \Omega_4 &= S_4 + \{ S_1 S_3 \} + \boxed{\frac{1}{2} \{ S_2 \} + \frac{1}{2} \{ S_1^2 S_2 \} + \frac{1}{4!} \{ S_1 \}^4}, \\ \Omega_5 &= \dots \end{aligned} \quad (18)$$

From Eq. (18), it is clear that when truncating after the S_2 cluster, we still include the parts of Ω_3 and Ω_4 that can be written as combinations of S_1 and S_2 operators, i.e., the terms in boxes above. This is the couple cluster singles and doubles method. The products of the S operators in the expansion are further discussed in Sec. III C. More details can be found in Ref. 45. There are two clear advantages of this truncation scheme. First, the probably most important triple and quadruple excitations, see, e.g., the bench-mark study on the beryllium atom,⁴⁶ are now included in a scheme that is much less computationally demanding than the calculation of all such excitations. Second, and this is in contrast to the scheme indicated in Eq. (14), the inclusion of the $\{ S_i S_j \}$ products makes the coupled-cluster method size extensive also in its truncated version.

In the following, we will investigate the performance of the coupled cluster method when including all S_1 and S_2 terms in Eq. (18) (the expressions in boxes), i.e., the CCSD method. Although the practical implementation is different, the present study includes the same effects as the implementation for atoms by Salomonson and Öster,⁴⁵ where more details about the method can be found.

III. IMPLEMENTATION

A. Single-particle treatment

The Hamiltonian for a single particle confined in a circularly symmetric potential reads

$$\hat{h} = \frac{\hat{\mathbf{p}}^2}{2m^*} + \hat{u}_c(r), \quad (19)$$

where the effective electron mass is denoted with m^* . With a pure harmonic confinement we have

$$\hat{u}_c(r) = \frac{1}{2}m^*\omega^2 r^2. \quad (20)$$

This is the confining potential used in all numerical results in the present study but any circularly symmetric confinement can be used in the developed computer code.

The single-particle wave functions separate in polar coordinates as

$$\Psi_{nm_l m_s}(r, \phi) = u_{nm_l m_s}(r) e^{im_l \phi} |m_s\rangle. \quad (21)$$

We expand the radial part of the wave functions in so called B-splines labeled B_i with coefficients c_i , i.e.,

$$u_{nm_l m_s}(r) = \sum_{i=1} c_i B_i(r). \quad (22)$$

B splines are piecewise polynomials of a chosen order k , defined on a so-called knot sequence and they form a complete set for the linear space defined by the knot sequence and the polynomial order.⁴⁷ Here, we have used 40 points in the knot sequence, distributed by the use of an arcsin function. The last knot point, defining the boundary of the box to which we limit our problem, is scaled with the potential strength through the harmonic oscillator length unit $\sqrt{\hbar/(m^*\omega)}$. For example, with $\hbar\omega \approx 11.857$ meV (which corresponds 1 a.u.* for GaAs, see Sec. IV), the last knot point is located at $r \sim 70$ nm. The polynomial order is ten and combined with the knot sequence this yields 29 radial basis functions, $u_{nm_l m_s}(r)$, for each combination (m_l, m_s) . The lower-energy basis functions are physical states, while the higher ones are mainly determined by the box. The unphysical higher-energy states are, however, still essential for the completeness of the basis set.

Equations (21) and (22) imply that the one-particle Schrödinger equation (19) can be written as a matrix equation:

$$\mathbf{h}\mathbf{c} = \epsilon\mathbf{B}\mathbf{c}, \quad (23)$$

where $h_{ij} = \langle B_i | e^{im_l \theta} | \hat{h} | B_j | e^{im_l \theta} \rangle$ and $B_{ij} = \langle B_i | B_j \rangle$.

Equation (23) is a generalized eigenvalue problem that can be solved with standard numerical routines. The integrals in Eq. (23) are calculated with Gaussian quadrature. B splines are piecewise polynomials, and since also the potential is in polynomial form in Eq. (19), essentially no numerical error is produced in the integration.

B. The Coulomb interaction

The perturbation V in Eq. (2) will include the electron-electron interaction not accounted for in H_0 . It can be the full Coulomb interaction or the difference between that and some mean-field approximation. In either case, we need a suitable way of dealing with the Coulomb interaction in two dimensions. As suggested by Cohl *et al.*,⁴⁸ the inverse radial distance can be expanded in cylindrical coordinates (R, ϕ, z) as

$$\frac{1}{|\mathbf{r}_1 - \mathbf{r}_2|} = \frac{1}{\pi\sqrt{R_1 R_2}} \sum_{m=-\infty}^{\infty} Q_{m-\frac{1}{2}}(\chi) e^{im(\phi_1 - \phi_2)}, \quad (24)$$

where

$$\chi = \frac{R_1^2 + R_2^2 + (z_1 - z_2)^2}{2R_1 R_2}. \quad (25)$$

Assuming a two-dimensional confinement we set $z_1 = z_2$ in Eq. (25). The $Q_{m-\frac{1}{2}}(\chi)$ functions are Legendre functions of the second kind and half-integer degree. We evaluate them using a modified version of software DTORH.f described in Ref. 49.

Using Eqs. (21) and (24), we can write the electron-electron interaction matrix element as

$$\begin{aligned} & \frac{e^2}{4\pi\epsilon_r\epsilon_0} \langle ab | \frac{1}{r_{12}} | cd \rangle \\ &= \langle ab | \frac{1}{\hat{r}_{12}} | cd \rangle = \frac{e^2}{4\pi\epsilon_r\epsilon_0} \langle u_a(r_i) u_b(r_j) | \frac{Q_{m-\frac{1}{2}}(\chi)}{\pi\sqrt{r_i r_j}} \\ & \quad \times | u_c(r_i) u_d(r_j) \rangle \langle e^{im_l^a \phi_i} e^{im_l^b \phi_j} | \sum_{m=-\infty}^{\infty} e^{im(\phi_i - \phi_j)} \\ & \quad \times | e^{im_l^c \phi_i} e^{im_l^d \phi_j} \rangle \langle m_s^a | m_s^c \rangle \langle m_s^b | m_s^d \rangle. \end{aligned} \quad (26)$$

Note that the angular (ϕ) integration in Eq. (26) yields a nonzero result only if $m = m_l^a - m_l^c = m_l^d - m_l^b$. This determines the degree m of the Legendre function in the radial part of Eq. (26). It is also clear from Eq. (26) that the electron-electron matrix element equals zero if orbital a and c or orbitals b and d have different spin directions.

If V in Eq. (2) has to account for the full electron-electron interaction, as it does when the single-particle Hamiltonian just includes the external confinement potential, Eq. (20), it might be difficult to obtain convergence of the iterative solutions of Eq. (8). At least, this is expected for weak external confinement and for many-electron dots. A remedy is then to start from a Hamiltonian H_0 that already includes the bulk of the electron-electron interaction. This can for instance be done by using the Hartree-Fock or local density approximation methods. Such options have been implemented to the present CCSD routine, however, no results using it are shown in this work.

C. Many-body treatment

Equipped with a finite representation of Q space it is possible to construct the S_n operators, and thus also the wave operator Ω . We now use the coupled cluster singles and doubles truncation of the possible excitations, i.e., only the terms in the boxes in Eq. (18) are kept. We start from Eq. (16) and note that for a model space built from a single Slater determinant, the $\chi P V \Omega P$ term is fully canceled by the unlinked diagrams from the $Q V \Omega P$ term. Only the $Q V \Omega P$ term remains thus on the right-hand side of Eq. (16). Starting with $\Omega^{(1)} = 1$ and $\chi^{(1)} = 0$, we can write the recursion relation for the the S_1 amplitudes as

$$\begin{aligned} \langle \alpha_r^r | S_1 | \alpha \rangle^{i+1} &= \frac{1}{\epsilon_a - \epsilon_r} \langle \alpha^r | V_1 + V S_1 + V S_2 + \frac{1}{2!} V \{ S_1^2 \} \\ & \quad + V_2 \{ S_1 S_2 \} + \frac{1}{3!} V_2 \{ S_1^3 \} | \alpha \rangle^i \end{aligned} \quad (27)$$

and for the S_2 -amplitudes,

$$\begin{aligned} \langle \alpha_{ab}^{rs} | S_2 | \alpha \rangle^{i+1} = & \frac{1}{\epsilon_a + \epsilon_b - \epsilon_r - \epsilon_s} \langle \alpha_{ab}^{rs} | V_2 + V_2 S_1 + V S_2 \\ & + \frac{1}{2!} V_2 \{ S_1^2 \} + V \{ S_1 S_2 \} + \frac{1}{3!} V_2 \{ S_1^3 \} \\ & + \frac{1}{2!} V_2 \{ S_2^2 \} + \frac{1}{2!} V_2 \{ S_1^2 S_2 \} + \frac{1}{4!} V_2 \{ S_1^4 \} | \alpha \rangle^i, \end{aligned} \quad (28)$$

where only connected contributions should be kept on the right-hand side. Here, $V = V_1 + V_2$ is the total perturbation, V_1 is the part of the perturbation that can be written as a one-particle operator and V_2 is the part of the perturbation that can be written as a two-particle operator. The index i denotes the iteration number. It is related, but not equal, to the order in the perturbation expansion. The quoted figures in Sec. IV are always self-consistent with respect to Eqs. (27) and (28). Note that, e.g., the single excitation cluster S_1 , see Eq. (27), is built from up single, double and triple excitations. As an example, we note that the included triples are those that can be written as disconnected singles connected by a perturbation V_2 [the last term on the second line of Eq. (27)] as well as combinations of singles and doubles connected by V_2 [second term on the last line of Eq. (27)]. These are so-called *intermediate* triple excitations. In a similar way, also intermediate triples and quadruples contribute to S_2 .

Finally, it is appropriate to comment on the difference between the two-dimensional many-body procedure and the more studied three-dimensional case, especially with respect to the angular integration. The angular momentum algebra is considerably simplified in two spatial dimensions compared to three. In two dimensions, an orbital is defined by only three quantum numbers. With polar coordinates these are the radial quantum number n the angular quantum number m_ℓ and the

spin direction m_s . The radial functions $u_{nm_\ell m_s}(r)$, Eq. (21), depend on two of these quantum numbers, n, m_ℓ , while an additional dependence on m_s only arises in case an external magnetic field is applied to the dot. In three dimensions, the desired total angular momentum has to be constructed through a linear combination of the different magnetic components of the orbitals. In spite of the advanced formalisms (e.g., Racah algebra) developed in order to avoid explicit summation over magnetic sub-states, the angular integration often gets rather cumbersome, at least for general open shell configurations. In two dimensions, there is only place for one particle in each spatial orbital and any state with maximized total spin can be treated as a closed shell configuration is handled in three dimensions.

IV. RESULTS

In our numerical studies, we use $m^* = 0.067 m_e$ and $\epsilon_r = 12.4$ corresponding to the bulk value in GaAs. The effective energy unit a.u.* corresponds then to approximately 11.857 meV and the effective Bohr radius to $a_0^* \approx 9.794$ nm.

A. Validation

Table I compares the present results with those obtained by full configuration interaction (FCI), Refs. 18,21, and 51, for 2–6 and 8 electrons. The couple-cluster equations are here solved with H_0 , cf. Eqs. (2) and (3), being the pure harmonic oscillator Hamiltonian and V accounting for the full electron–electron interaction. The purpose of Table I is on the one hand to compare with calculations that include exactly the same physical effects. Such a comparison can in principle only be done for two electrons due to the truncation at the S_3 clusters in the CCSD method. A second purpose is to investigate the accuracy and basis set convergence for more than two electrons and for confinement strengths close to the region of interest.

TABLE I. Comparison between the coupled cluster singles and doubles (CCSD) method and full configuration interaction (FCI) according to Kvaal²¹ as well as to Rontani *et al.*¹⁸ The basis is in all three cases defined by the one-electron harmonic oscillator Hamiltonian and is truncated after a specific number of major oscillator shells $R = 2n + |m_\ell|$. Energies are given in units of $\hbar\omega$ and the number of confined electrons is 2–6 and 8.

	$ 2SM_L\rangle$	$\hbar\omega(\text{meV})$	Basis set	CCSD	FCI	
				This work	Kvaal	Rontani <i>et al.</i>
$N = 2$	00)	11.857 20	$R = 7$	3.009 234	3.009 236 ^a	
		2.964 301	$R = 7$	3.729 323	3.729 324 ^a	3.729 5
		0.329 366 8	$R = 5$	5.784 651		5.785 0
		0.185 268 8	$R = 7$	6.618 089		6.618 5
$N = 3$	11)	11.857 20	$R = 10$	6.367 73	6.365 615 ^b	
		2.964 301	$R = 7$	8.176 35	8.166 708 ^b	8.167 1
$N = 4$	20)	2.964 301	$R = 7$	13.635		13.626
$N = 5$	11)	2.964 301	$R = 7$	20.346 7		20.33
$N = 6$	00)	2.964 301	$R = 5$	28.016 1	28.033 0 ^c	28.03
			$R = 7$	27.975 1		27.98
			$R = 15$	27.939 0		
$N = 8$	20)	2.964 301	$R = 5$	47.138 01		47.14
			$R = 15$	46.679 60		

^aSimen Kvaal.²¹

^bSimen Kvaal⁵⁰ obtained with the software in Ref. 21.

^cPatrick Merlot⁵¹ using the software in Ref. 21.

The basis set used is truncated using the shells truncation parameter, $R = 2n + |m_l|$. This truncation scheme is a common choice in numerical studies,^{18,21} and the motivation to study convergence as a function of this parameter is that the harmonic oscillator single-particle energies are given by $\epsilon_{nm_\ell} = (2n + |m_\ell| + 1)\hbar\omega$.

For two electrons, $N = 2$, both the CCSD and the FCI method take all electron-electron effects into account and the accuracy is thus only limited by the size of the basis set and the numerical procedure. When comparing the $N = 2$ results produced with identical basis sets in Table I, we note that our values differ from those produced by Kvaal²¹ at most in the seventh digit, while those by Rontani *et al.*¹⁸ differ in the fifth digit. The computer code developed by Kvaal²¹ is benchmarked to machine precision with exact results and it is reasonable to believe that its numerical accuracy is the highest. The leading numerical errors in the present implementation are due to the precision in the $Q_{m-1/2}$ functions produced by DTORH1.f and their integration in Eq. (26). For more than two electrons, these numerical errors are much smaller than the errors introduced through truncations and are of no significance. For the the remaining part of Table I, we restrict the display of our results to six digits.

Since coupled-cluster equations are solved iteratively, convergence is never guaranteed. The key parameter here is the strength of the electron-electron interaction relative to the confinement provided by the harmonic oscillator potential. One way to quantify this is through the dimensionless parameter

$$\lambda = \sqrt{\frac{\hbar}{\omega m^*}} \frac{1}{a_0^*}, \quad (29)$$

where $a_0^* = a_0 \epsilon_r m_e / m^*$ is the effective Bohr radius obtained by a material dependent scaling of the Bohr radius (a_0) and $\sqrt{\frac{\hbar}{\omega m^*}}$ is the typical harmonic oscillator length unit. Large λ values correspond to a weaker confinement and an increased relative importance of the electron-electron interaction. The confinement strengths chosen for $N = 2$ in Table I correspond to $\lambda = 1$ ($\hbar\omega = 11.8572$ meV), $\lambda = 2, 6$ and, finally, $\lambda = 8$ ($\hbar\omega = 0.1852688$ meV). We note that for only two-electrons convergence is still obtained for this last confinement even though the full electron-electron interaction is here taken as the perturbation. We emphasize that this constitutes a truly nonperturbative case; the total energy is almost seven times as large as the strength of the confining potential.

Continuing to $N > 2$, we conclude from Table I that the largest relative error, calculated as the percentage of the total energy, arises for $N = 3$. Still the deviation is never larger than $\sim 1.5 \times 10^{-2}$ in units of $\hbar\omega$ or ~ 0.1 percent of the total energy. For six and eight electrons, we also increased the basis set significantly beyond what so far has been feasible with FCI. It is clear that the error made by the truncation of the coupled cluster expansion at the S_3 cluster operator is far smaller than the error made by truncating the basis set in the CI calculations.

Table I shows only results obtained with the whole electron-electron interaction taken as the perturbation. This was done in order to compare directly with the CI calculations. These typically use a pure harmonic oscillator basis set, which further is severely truncated. With this starting point, convergence

TABLE II. The importance of S_3 clusters and beyond. The present coupled cluster singles and dDoubles (CCSD) results are compared to full configuration interaction (FCI)^{21,50,51} results obtained with the same basis sets. For three electrons, the basis is for both methods truncated at $R = 2n + |m_l| = 7$, and with six electrons it is truncated at $R = 5$. These basis sets are *not* saturated, but the comparison unveils the level at which contributions beyond CCSD contribute, as function of the confinement strength. The values in parenthesis are the differences to the corresponding full CI value. Energies are given in units of $\hbar\omega$.

	$ 2SM_L\rangle$	$\hbar\omega(\text{meV})$	CCSD	Full CI
$N = 3$	11)	47.428 81	5.286 60 (+ 0.000 19)	5.286 40
		21.079 47	5.850 48 (+ 0.000 77)	5.849 71
		11.857 20	6.372 92 (+ 0.001 87)	6.371 06
		5.269 868	7.321 69 (+ 0.005 39)	7.316 30
		2.964 301	8.176 35 (+ 0.009 65)	8.166 70
		0.741 075 2	diverges	11.042 5
	30)	47.428 81	5.908 15 (+ 5×10^{-6})	5.908 14
		21.079 47	6.340 19 (+ 0.000 02)	6.340 17
		11.857 20	6.759 08 (+ 0.000 06)	6.759 03
		5.269 868	7.561 47 (+ 0.000 20)	7.561 28
0.741 075 2		11.051 4 (− 0.001 20)	11.052 6	
$N = 6$	00)	1185.720	11.197 9 (+ 8×10^{-7})	11.197 9
		47.428 81	15.562 4 (+ 0.000 62)	15.561 8
		11.857 20	20.260 9 (+ 0.003 71)	20.257 2
		2.964 301	28.016 1 (− 0.016 87)	28.033 0

of the coupled-cluster expansion for weaker confinements than $\hbar\omega = 2.964301$ meV, for $N > 2$ can be problematic. However, convergence can be obtained for a much wider range of confinement strengths with a better starting point: e.g., Hartree-Fock or Local density, but a meaningful comparison would then only be possible with untruncated, or at least converged, FCI calculations.

A strict limitation of the CCSD approach is the neglect of true triples, S_3 clusters, and beyond. For sufficiently weak confinements, this approximation will dominate the error. Table II shows a comparison between the CCSD and FCI methods for three and six electrons and for a large range of confinement strengths. The purpose is here to establish how important the limitation to S_1 and S_2 clusters is. The weakest possible confinement strengths that still lead to a converged coupled-cluster expansion in the one-particle harmonic oscillator basis have been used. We note that for $\hbar\omega \geq 11.85720$ meV, the CCSD method yields results accurate enough for most practical purposes. For $\hbar\omega = 2.964301$ meV ($\lambda = 2$), the error due to the neglected effects in the CCSD method is still so small that the possibility to use larger basis sets than in a CI calculation well compensates for the lack of triples and beyond. For $N = 3$ and $\hbar\omega = 0.7410752$ meV ($\lambda = 4$), the CCSD did not converge for the $|2SM_L 1\rangle = |11\rangle$ ground state. However, even for this weak confinement, the first excited state is still reproduced well. Generally, we see that this first excited state, which is not as localized as the ground state, is reproduced better than the ground state throughout the list of confinements strengths in Table II. Intuitively this makes sense, true triple excitations should be relatively more important for more localized states.

B. Comparison to other coupled cluster and Monte Carlo implementations

We now set out to compare the results of the present CCSD implementation to those obtained by Pedersen Lohne *et al.*³⁸ The referenced work presents calculations with the Diffusion Monte Carlo (DMC) method as well as with two different CCSD approaches. The first of these is similar to the one used here, although the primitive basis consists of analytical harmonic oscillator eigenstates instead of B splines. The other utilize a renormalized effective Coulomb interaction for improved convergence. This effective interaction has earlier been used in quantum dot CI calculations by Navrtil *et al.*⁵² Assuming that the DMC is near the exact result, or at least acting as an upper boundary to the exact result,⁵³ we can investigate the quality of the different CCSD implementations.

Table III compares first the results for the two-electron case. Since CCSD includes all one- and two-body interactions, differences compared to DMC are only expected to arise due to the truncation of the basis. The results from the two ordinary CCSD implementations are further expected to behave in the same way and produce similar results. However, as the routine from the present study produces a slow, smooth convergence in R , the Pedersen Lohne results show a spike in convergence between $R = 7$ and 9 for $\hbar\omega = 11.857$. This jump in convergence cannot be explained by neither the accuracy of the numerical routines, nor by the slight difference in the used basis. Closer investigations⁵⁰ and a comparison

to other (but unpublished) results produced using the same CCSD code,^{54,55} indicate that there might be a mistake in the tabulation in Ref. 38, and that the energies for $R = 9$ and above are misplaced from a different calculation. For $R < 9$, there is perfect agreement between the results in Ref. 38 and the tabulation in Ref. 54. Disregarding the $\hbar\omega = 11.857$ meV values with $R \geq 9$, the agreement between the present results and the referenced is to within a few units in the fifth decimal.

Also the results for six and twelve electrons seem to be incorrect for the truncations of $R \geq 9$, and the results are significantly higher in energy than the corresponding energies presented in this work. Although, for truncations at $R < 9$, we have agreement within a few thousands of a percent. The CCSD results from Refs. 54 and 55 for six and twelve electrons obtained with the harmonic oscillator basis also agree with the present results to within the same relative level for all tested values of R .

The Pedersen Lohne data imply that the use of the so-called effective interaction is required to obtain high-accuracy results. Due to this conclusion, they present more results using the effective interaction than using the bare one. Thus, in Table III, these results are also compared to ours. The energies produced in this way seem to be highly converged before $R = 10$, this is because a large part of the two-particle interaction for a larger basis is already included. In the case of two electrons, all energy contributions have already been accounted for in the initial step of forming the effective interaction in a larger basis,

TABLE III. Comparison to ground-state energies from the coupled cluster singles and doubles and diffusion Monte Carlo implementations by Pedersen Lohne *et al.*³⁸ The column labeled CCSD- V_{eff} is the CCSD method utilizing a so-called effective Coulomb interaction. The energies are given in a.u.* and $R = 2n + |m_l|$.

	$ 2SM_L\rangle$	$\hbar\omega(\text{meV})$	Basis set	This work	Pedersen Lohne <i>et al.</i> ^a		
				CCSD	CCSD	CCSD- V_{eff}	DMC
$N = 2$	00)	5.928 6	$R = 3$	1.673 837	1.673 874	1.659 772	
			$R = 9$	1.663 509	1.663 535	1.659 772	
			$R = 13$	1.662 218	1.662 244	1.659 772	
			$R = 19$	1.661 295	1.661 378	1.659 772	1.659 75(2)
	11.857	$R = 1$	3.152 164	3.152 329	3.000 000		
		$R = 3$	3.025 149	3.025 232	3.000 000		
		$R = 5$	3.013 554	3.013 627	3.000 000		
		$R = 7$	3.009 168	3.009 237	3.000 000		
		$R = 9$	3.006 873	3.000 895	3.000 000		
		$R = 15$	3.003 834	3.000 406	3.000 000		
$N = 6$	00)	3.320 0	$R = 9$	7.609 961		7.624 1	
			$R = 13$	7.605 555		7.624 7	7.600 1(1)
	5.928 6	$R = 9$	11.809 63		11.805 7		
		$R = 13$	11.800 93		11.805 5	11.788 8(2)	
	11.857	$R = 5$	20.260 45	20.260 893			
		$R = 9$	20.203 97	20.216 128	20.176 6		
		$R = 13$	20.188 18	20.199 986	20.174 6	20.159 7(2)	
$N = 12$	00)	3.320 0	$R = 9$	25.609 92		25.706 9	
			$R = 13$	25.593 84		25.707 4	25.635 6(1)
	5.928 6	$R = 9$	39.177 55		39.221 8		
		$R = 13$	39.141 25		39.219 7	39.159(1)	
	11.857	$R = 5$	66.448 68	65.452 006			
		$R = 9$	65.803 25	65.887 965	65.755 2		
	$R = 13$	65.741 07	65.825 018	65.744 9	65.700(1)		

^aThe R classification of the results from Ref. 38 has been changed to coincide with the definition of R used here.

enabling the perfect results displayed. For larger systems, additional contributions are added by the CCSD routine. Still, the present approach seems to generate better results for weak interactions and high electron numbers, but is inferior when applied to few electrons and strong potentials, possibly due to a dominance of pure two-electron effects in the latter. For $N = 12$ with $\hbar\omega = 5.9286$ and 3.3200 , we even get a lower energy than the corresponding Monte Carlo energies. However, it is difficult to determine which results are more correct here since the DMC energies only act as an upper bound, and the S_3 clusters (and beyond) that we do not include will probably be of increased importance for many particles in weak confinements. It is thus possible that CCSD exclude an important part of the energy contribution here. As previously seen in Table II, the missing higher-order clusters lead to a higher energy than the FCI energy for all but the weakest confinement in the $N = 3$ and 6 cases. This is consistent with the fact that the missing clusters (S_3 and beyond) will start to contribute to the energy in fourth order in a perturbation expansion and is thus expected to be negative, at least for sufficiently strong confinements where the contributions are steadily decreasing with perturbation order. The increasing magnitude of the error can be explained by the increasing importance of the omitted clusters when the confinement is decreasing and the number of particles are increasing.

C. Convergence of the basis

In Table IV, the convergence properties for the ground-state energies are displayed for different numbers of electrons as a function of the truncation parameter R . The confining potential is $\hbar\omega = 3.32$ meV, a strength previously studied with quantum Monte Carlo methods,²⁹ whereof both the variation(VMC) and diffusion(DMC) Monte Carlo energies are shown in Table IV for comparison. At $R = 15$, convergence is usually obtained down to the fifth digit. Compared to the VMC results, the CCSD seems to converge towards a slightly higher value for systems of less than four electrons and a lower value for higher electron numbers, while the DMC results always are lower than the CCSD's. To get a higher

degree of convergence, one could of course increase the basis size. Even though much larger basis sets can be used with CCSD than with CI, the calculation time still grows with the number of particles and with the size of the basis set. Extrapolation of the results to infinitely large basis sets is then often an efficient strategy. Many elaborate strategies can be envisaged here, e.g., adjusting the size of the basis set during the iterations. One can, for example, obtain convergence in a limited basis and then systematically increase it, or one can filter the contributions and only keep those that are estimated to contribute over a certain level. Here, we restrict ourselves to a brief discussion of the potential gain of extrapolation.

We start by considering the case of six electrons confined in a $\hbar\omega = 11.85720$ meV harmonic oscillator potential. Instead of truncating the basis by the oscillatory shell number R , we now truncate it by the one electron n and $|m_l|$ quantum numbers. The total number of included states, excluding there being two spin directions, is used as a quantification of the basis size, i.e., $n(2|m_l| + 1)$. In Figs. 1 and 2, we can see the convergence properties of this basis truncation scheme. Note that the data points in the two figures are identical, but the convergence properties are displayed differently. In Fig. 1, $\max(n)$ is kept fixed at some value and the plotted lines show the energy convergence when increasing $\max(|m_l|)$. In the same way, Fig. 2 displays this for a fixed $\max(|m_l|)$ and increasing $\max(n)$. Figure 1 clearly shows that the energies are already fairly converged when the basis is truncated at $|m_l| = 9$, and that there is probably very little to gain from going higher than $|m_l| = 10$. Viewing these figures, one can conclude that the previously obtained energy from truncating at $R = 13$, $E = 20.18818$ a.u.*, is apparently not fully converged. In fact neither is the energy for the largest basis sets showed in Figs. 1 and 2. To get the properly converged energy, we need to go to $\max(n) > 15$ and $\max(|m_l|) > 10$. Increasing the $\max(n)$ quantum number will also increase the computation time, and the scaling is quite unfavorable. To some extent, this could be counteracted by reducing the $\max(|m_l|)$ quantum number, while increasing $\max(n)$ and then extrapolate the energy with respect to $|m_l|$, using the results

TABLE IV. The $R = 2n + |m_l|$ convergence for the 2–8 electron ground states for a confining potential corresponding to $\hbar\omega = 3.32$ meV. CCSD energies are compared to results from the variational and diffusion quantum Monte Carlo methods. The energies are given in a.u.*

R	$2e^-$	$3e^-$	$4e^-$	$5e^-$	$6e^-$	$7e^-$	$8e^-$
5	1.025 44	2.240 45	3.726 52	5.553 17	7.626 40	10.091 3	12.806 5
6	1.024 70	2.239 24	3.724 39	5.548 90	7.619 42	10.062 4	12.728 4
7	1.024 20	2.238 46	3.722 10	5.546 29	7.614 96	10.054 1	12.713 2
8	1.023 83	2.237 91	3.722 07	5.544 54	7.612 07	10.049 8	12.706 7
9	1.023 55	2.237 50	3.721 40	5.543 27	7.610 00	10.046 9	12.702 7
10	1.023 33	2.237 19	3.720 89	5.542 34	7.608 46	10.044 8	12.700 0
11	1.023 15	2.236 94	3.720 50	5.541 61	7.607 28	10.043 1	12.697 9
12	1.023 01	2.236 74	3.720 18	5.541 02	7.606 33	10.041 9	12.696 2
13	1.022 89	2.236 57	3.719 91	5.540 54	7.605 57	10.040 8	12.694 9
14	1.022 78	2.236 43	3.719 69	5.540 14	7.604 93	10.040 0	12.693 9
15	1.022 69	2.236 31	3.719 50	5.539 79	7.604 38	10.039 3	12.693 0
QMC ^a	1.021 65(1)	2.239 5(1)	3.719 4(1)	5.544 8(1)	7.610 4(1)	10.049 9(1)	12.708 7(1)
QMC ^b	1.021 64(1)	2.233 9(1)	3.714 5(1)	5.533 8(1)	7.600 1(1)	10.034 2(1)	12.690 0(1)

^aVariation Monte Carlo, Pederiva *et al.*²⁹

^bDiffusion Monte Carlo, Pederiva *et al.*²⁹

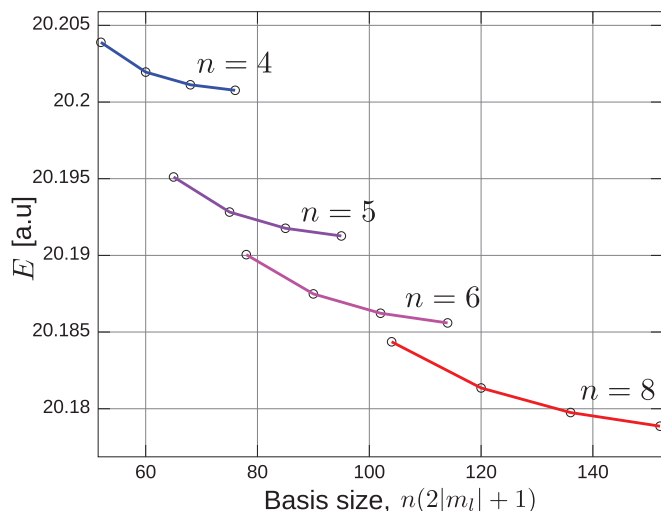


FIG. 1. (Color online) Total energies for a six electron $\hbar\omega = 11.85720$ meV harmonic oscillator potential, truncating the basis by the n and $|m_l|$ quantum numbers, displaying the convergence in the $|m_l|$ dimension, for $n = [4, 5, 6, 8]$. The data points in this figure are identical to the ones in Fig. 2.

from a few low values of $|m_l|$. However, care has to be taken to use the converged basis in the n -dimension. Which in our case is ensured by using all the radial states in the B-spline basis, guaranteeing convergence due to the completeness of the basis. The high-energy states will not be the correct physical one-particle harmonic oscillator states since our primitive basis, the B splines, is finite. However, this is not a problem if the entire set is included, since the B splines form a complete basis in the numerical box. The extrapolated energies in the $|m_l|$ expansion are obtained through a linear regression fit assuming the relation

$$\ln [E(|m_\ell|) - E(|m_\ell| + 1)] = K \ln(|m_\ell| + 1) + C, \quad (30)$$

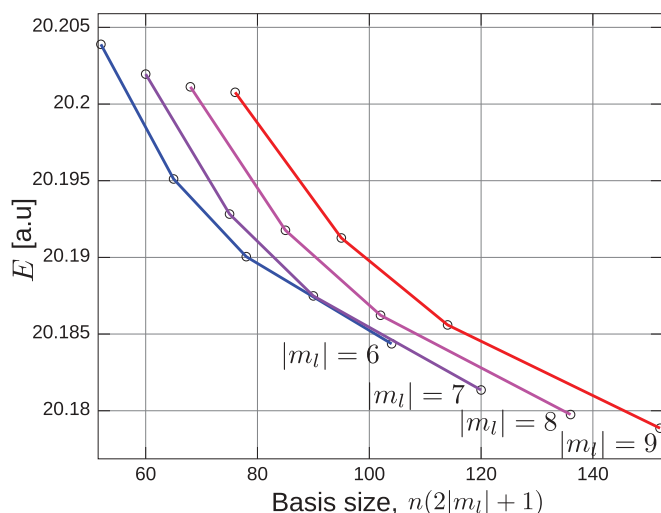


FIG. 2. (Color online) Total energies for a six electron $\hbar\omega = 11.85720$ meV harmonic oscillator potential, truncating the basis by the n and $|m_l|$ quantum numbers, displaying the convergence in the n dimension, for $|m_l| = [6, 7, 8, 9]$. The data points in this figure are identical to the ones in Fig. 1.

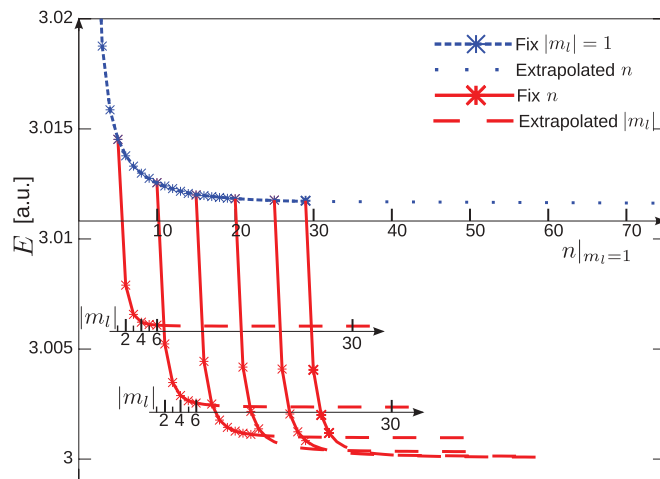


FIG. 3. (Color online) The energy for a two electron $\hbar\omega = 11.85720$ meV harmonic oscillator potential. The stars are results from running the CCSD routine using n and $|m_l|$ truncation. The stars on the finely dashed (blue) line are truncated at $|m_l| = 1$ and for the set $n = [2 : 20, 25, 29]$, with the line being a fit to match these. The stars on the full (red) lines are truncated at the n value from which they start, i.e., $n = [5, 10, 15, 20, 25, 29]$, with an increasing $|m_l|$ value. The dashed lines continuing from the full line and the dotted line continuing from the finely dashed line are the extrapolated energies in the corresponding dimensions. The final extrapolated energy for $n = 29$ and $|m_l| = 30$ is $E = 3.000\,089\,638$ a.u.*

where $E(|m_\ell|)$ is the energy obtained with the one-particle basis cut at $\max(|m_\ell|) = |m_\ell|$ and K and C are the constants to be found from the fit.

In Fig. 3, the extrapolation in the $|m_l|$ dimension is demonstrated for the two-electron case. The figure shows the need of a basis that expands in both quantum numbers, since neither a low $|m_l|$, high n ; nor a high $|m_l|$, low n truncation is adequate. The fit seems to match the behavior in the $|m_l|$ dimension and at $\max(|m_l|) = 30$ the energies seem completely converged. Since this system only has two electrons, the computation time for the full radial basis, all basis functions with $n \leq 29$, is acceptable. The figure clearly shows a convergence in the extrapolated values towards $E = 3$ a.u.*, the energy expected from analytical calculations.⁵⁶ Our final result $E = 3.000\,089\,64$ a.u.* can be compared to what we got previously from truncation at $R = 15$, $E = 3.003\,834$ a.u.*. The error is reduced by a factor of 40 and is close to the errors in the DMC results presented earlier. It is worth to note that this method of increasing accuracy is due to the fact that the B splines form a complete radial basis and would have required a similar extrapolation in the $|m_l|$ dimension if any other basis set had been used.

Another option would be to perform the same kind of extrapolation for the n or R quantum numbers, however, no sufficiently good relation has yet been found that accurately could mimic the convergence behavior in these two dimensions. Knowledge regarding these convergence properties might also allow us to form better truncation schemes than the major oscillatory shell truncation. This scheme might include too many low n , high $|m_l|$ states that only have a small effect on the energy. Also, high n states might be of greater importance than earlier expected.

V. CONCLUSIONS

In conclusion, the coupled cluster singles and doubles approach is shown to be a very powerful method for at least up to twelve electrons confined in a two-dimensional harmonic oscillator potential. The results are, for practical purposes, exact for $\lambda \leq 1$ when comparing with FCI. Further, given $\lambda = 2$, the error is never larger than $\sim 1.5 \times 10^{-2}$ in units of $\hbar\omega$. The possibility to use much larger basis sets than in FCI calculations for $N \geq 6$, is shown to be of considerable importance. The errors introduced by truncating the basis sets in FCI-calculations are in many cases much larger than the error made by truncating some of the triple and quadruple excitations as done in CCSD. Moreover, when comparing with a diffusion Monte Carlo study, for a potential strength close to what is estimated from the experiment by Tarucha *et al.*,¹ the errors in the ground-state energies for up to eight electrons are shown to be on the same level or less than the differences between variational and diffusion Monte Carlo results. In comparison to the CCSD routine by Pedersen Lohne,³⁸ the present implementation seems to yield better

results when using the standard Coulomb interaction, and also when comparing to the results obtained from using an effective interaction in Ref. 38. Some underestimation of the energy does occur for high N systems and may be due to the increased importance of the clusters that have been neglected. The use of different truncation schemes than the shell truncation has also been shown to be a promising possibility, and by utilizing extrapolations in the $|m_l|$ dimension, the error in the two electron energy was reduced by a factor of 40, compared to truncating at $R = 15$. These results hold promise that the method can be used for the extraction of reliable information from experiments in future studies.

ACKNOWLEDGMENTS

Financial support from the Swedish Research Council (VR) and from the Göran Gustafsson Foundation is gratefully acknowledged. We also want to thank Simen Kvaal for several discussions and for providing us with unpublished configuration interaction results.

-
- ¹S. Tarucha, D. Austing, T. Honda, R. J. van der Hage, and L. P. Kouwenhoven, *Phys. Rev. Lett.* **77**, 3613 (1996).
- ²P. Matagne and J.-P. Leburton, *Phys. Rev. B* **65**, 155311 (2002).
- ³D. V. Melnikov, P. Matagne, J.-P. Leburton, D. G. Austing, G. Yu, S. T. cha, J. Fettig, and N. Sobh, *Phys. Rev. B* **72**, 085331 (2005).
- ⁴M. Koskinen, M. Manninen, and S. M. Reimann, *Phys. Rev. Lett.* **79**, 1389 (1997).
- ⁵M. Macucci, K. Hess, and G. J. Iafrate, *Phys. Rev. B* **55**, R4879 (1997).
- ⁶I. H. Lee, V. Rao, R. M. Martin, and J. P. Leburton, *Phys. Rev. B* **57**, 9035 (1998).
- ⁷M. Fujito, A. Natori, and H. Yasunaga, *Phys. Rev. B* **53**, 9952 (1996).
- ⁸S. Bednarek, B. Szafran, and J. Adamowski, *Phys. Rev. B* **59**, 13036 (1999).
- ⁹C. Yannouleas and U. Landman, *Phys. Rev. Lett.* **82**, 5325 (1999).
- ¹⁰U. D. Giovannini, F. Cavaliere, R. Cenni, M. Sassetti, and B. Kramer, *Phys. Rev. B* **77**, 035325 (2008).
- ¹¹S. M. Reimann and M. Manninen, *Rev. Mod. Phys.* **74**, 1283 (2002).
- ¹²P. Matagne, J. P. Leburton, D. G. Austing, and S. Tarucha, *Phys. Rev. B* **65**, 085325 (2002).
- ¹³N. A. Bruce and P. A. Maksym, *Phys. Rev. B* **61**, 4718 (2000).
- ¹⁴B. Szafran, S. Bednarek, and J. Adamowski, *Phys. Rev. B* **67**, 115323 (2003).
- ¹⁵S. M. Reimann, M. Koskinen, and M. Manninen, *Phys. Rev. B* **62**, 8108 (2000).
- ¹⁶S. A. Mikhailov, *Phys. Rev. B* **65**, 115312 (2002).
- ¹⁷S. A. Mikhailov, *Phys. Rev. B* **66**, 153313 (2002).
- ¹⁸M. Rontani, C. Cavazzoni, D. Bellucci, and G. Goldoni, *J. Chem. Phys.* **124**, 124102 (2006).
- ¹⁹V. Popsueva, R. Nepstad, T. Birkeland, M. Førre, J. P. Hansen, E. Lindroth, and E. Waltersson, *Phys. Rev. B* **76**, 035303 (2007).
- ²⁰E. Waltersson, E. Lindroth, I. Pilskog, and J. P. Hansen, *Phys. Rev. B* **79**, 115318 (2009).
- ²¹S. Kvaal, *Phys. Rev. B* **80**, 045321 (2009).
- ²²L. Sælen, E. Waltersson, J. P. Hansen, and E. Lindroth, *Phys. Rev. B* **81**, 033303 (2010).
- ²³R. J. Bartlett, *Annu. Rev. Phys. Chem.* **32**, 359 (1981).
- ²⁴H. Saarikoski and A. Harju, *Phys. Rev. Lett.* **94**, 246803 (2005).
- ²⁵R. Egger, W. Häusler, C. H. Mak, and H. Grabert, *Phys. Rev. Lett.* **82**, 3320 (1999).
- ²⁶R. Egger, W. Häusler, C. H. Mak, and H. Grabert, *Phys. Rev. Lett.* **83**, 462 (1999).
- ²⁷F. Pederiva, C. J. Umrigar, and E. Lipparini, *Phys. Rev. B* **62**, 8120 (2000).
- ²⁸A. J. Williamson, J. C. Grossman, R. Q. Hood, A. Puzder, and G. Galli, *Phys. Rev. Lett.* **89**, 196803 (2002).
- ²⁹F. Pederiva, C. J. Umrigar, and E. Lipparini, *Phys. Rev. B* **68**, 089901 (2003).
- ³⁰A. Ghosal and A. D. Güçlü, *Nat. Phys.* **2**, 336 (2006).
- ³¹S. Weiss and R. Egger, *Phys. Rev. B* **72**, 245301 (2005).
- ³²L. Zeng, W. Geist, W. Y. Ruan, C. J. Umrigar, and M. Y. Chou, *Phys. Rev. B* **79**, 235334 (2009).
- ³³W. M. C. Foulkes, L. Mitas, R. J. Needs, and G. Rajagopal, *Rev. Mod. Phys.* **73**, 33 (2001).
- ³⁴C. Sloggett and O. P. Sushkov, *Phys. Rev. B* **71**, 235326 (2005).
- ³⁵E. Waltersson and E. Lindroth, *Phys. Rev. B* **76**, 045314 (2007).
- ³⁶T. M. Henderson, K. Runge, and R. J. Bartlett, *Chem. Phys. Lett.* **337**, 138 (2001).
- ³⁷I. Heidari, S. Pal, B. S. Pujari, and D. G. Kanhere, *J. Chem. Phys.* **127**, 114708 (2007).
- ³⁸M. Pedersen Lohne, G. Hagen, M. Hjorth-Jensen, S. Kvaal, and F. Pederiva, *Phys. Rev. B* **84**, 115302 (2011).
- ³⁹F. Coester and H. Kümmel, *Nucl. Phys.* **17**, 477 (1960).
- ⁴⁰R. J. Bartlett and M. Musiał, *Rev. Mod. Phys.* **79**, 291 (2007).
- ⁴¹I. Lindgren and J. Morrison, *Atomic Many-Body Theory*, Series on Atoms and Plasmas, 2nd ed. (Springer-Verlag, New York, Berlin, Heidelberg, 1986).
- ⁴²I. Lindgren, *J. Phys. B: At. Mol. Opt. Phys.* **7**, 2441 (1974).
- ⁴³C. Bloch, *Nucl. Phys.* **6**, 329 (1958).
- ⁴⁴I. Lindgren, *Int. J. Q. Chem. S* **12**, 33 (1978).
- ⁴⁵S. Salomonson and P. Öster, *Phys. Rev. A* **41**, 4670 (1990).

- ⁴⁶A.-M. Mårtensson-Pendrill, S. A. Alexander, L. Adamowicz, N. Oliphant, J. Olsen, P. Öster, H. M. Quiney, S. Salomonson, and D. Sundholm, *Phys. Rev. A* **43**, 3355 (1991).
- ⁴⁷C. deBoor, *A Practical Guide to Splines* (Springer-Verlag, New York, 1978).
- ⁴⁸H. S. Cohl, A. R. P. Rau, J. E. Tohline, D. A. Browne, J. E. Cazes, and E. I. Barnes, *Phys. Rev. A* **64**, 052509 (2001).
- ⁴⁹J. Segura and A. Gil, *Comp. Phys. Comm.* **124**, 104 (1999).
- ⁵⁰S. Kvaal (private communication).
- ⁵¹P. Merlot, Master Thesis, University of Oslo, 2009. CI results are produced using the software written by Kvaal, Ref. 21.
- ⁵²K. Varga, P. Navratil, J. Usukura, and Y. Suzuki, *Phys. Rev. B* **63**, 205308 (2001).
- ⁵³D. M. Ceperley, in *Proceedings of the International School of Physics “Enrico Fermi”*, edited by G. F. Giuliani and G. Vignale (IOS Press, Amsterdam, 2004), pp. 3–42, Vol. 157.
- ⁵⁴M. P. Lohne, Master Thesis, University of Oslo, 2010. CCSD results are produced using the software in Ref. 38.
- ⁵⁵M. H. Jørgensen, Master Thesis, University of Oslo, 2011. CCSD results are produced using the software in Ref. 38.
- ⁵⁶M. Taut, *J. Phys. A* **27**, 1045 (1994).